Drivers of interannual variability in virioplankton abundance at the coastal Western Antarctic Peninsula and the potential effects of climate change

Claire Evans[1,†]*, Joost Brandsma[1,‡], David W. Pond[2,+], Hugh J. Venables[2], Michael P. Meredith[2], Harry J. Witte[1], Sharon Stammerjohn[3], William H. Wilson[4], Andrew Clarke[2], Corina P. D. Brussaard[1,5]

[1] Department of Biological Oceanography, Royal Netherlands Institute for Sea Research, PO Box 59, 1790 AB Den Burg, Texel, The Netherlands.

[2] British Antarctic Survey, Natural Environmental Research Council, High Cross, Madingley Road, Cambridge, CB3 0ET, United Kingdom.

[3] Institute of Arctic and Alpine Research, University of Colorado, Boulder, CO, United States of America.

[4] Sir Alister Hardy Foundation for Ocean Science, The Laboratory, Citadel Hill, Plymouth, PL1 2PB, United Kingdom.

[5]Aquatic Microbiology, Institute for Biodiversity and Ecosystem Dynamics, University of Amsterdam, P.O. Box 94248, 1090 GE Amsterdam, The Netherlands.

[†] present address: Ocean Biogeochemistry & Ecosystems Research Group, National Oceanography Centre, Southampton, European Way, Southampton, SO14 3ZH, United Kingdom.

[‡] present address: Clinical and Experimental Sciences, Faculty of Medicine, University of Southampton, Southampton, SO16 6YD, United Kingdom.

[+] present address: Scottish Association for Marine Sciences, Scottish Marine Institute, Oban, Argyll, PA37 1QA, United Kingdom.

[*] Corresponding author: Claire Evans, Ocean Biogeochemistry & Ecosystems Research Group, National Oceanography Centre, European Way, Southampton, SO14 3ZH, United Kingdom.

E-mail: claire.evans@noc.ac.uk; tel: +44 (0)2380 596338; fax: +44 (0)2380 596247.

Running title: Viruses in Antarctic coastal waters

Summary

An eight year time-series in the Western Antarctic Peninsula (WAP) with an approximately weekly sampling frequency was used to elucidate changes in virioplankton abundance and their drivers in this climatically-sensitive region. Virioplankton abundances at the coastal WAP show a pronounced seasonal cycle with interannual variability in the timing and magnitude of the summer maxima. Bacterioplankton abundance is the most influential driving factor of the virioplankton, and exhibit closely coupled dynamics. Sea ice cover and duration predetermine levels of phytoplankton stock and thus, influence virioplankton by dictating the substrates available to the bacterioplankton. However, variations in the composition of the phytoplankton community and particularly the prominence of Diatoms inferred from silicate drawdown, drive inter-annual differences in the magnitude of the virioplankton bloom; likely again mediated through changes in the bacterioplankton. Our findings suggest that future warming within the WAP will cause changes in sea ice that will influence viruses and their microbial hosts through changes in the timing, magnitude and composition of the phytoplankton bloom. Thus the flow of matter and energy through the viral shunt may be decreased with consequences for the Antarctic food web and element cycling.

Introduction

Viruses are abundant and active components of seawater that primarily infect the numerically dominant bacterioplankton and eukaryotic marine microbes (Brussaard, 2004; Weinbauer, 2004). As host-specific pathogens they exert control over assemblage composition (Brussaard, 2004; Suttle, 2005), and via gene transfer may serve as genetic reservoirs for marine microbes (Dinsdale *et al*., 2008). Virus-mediated lysis of host cells generates substrates for bacterioplankton, sequestering matter and energy in the microbial component of marine food webs (Middelboe, 2000; Suttle, 2007; Sheik *et al*., 2014). Thus, viral activity affects the productivity of higher tropic levels and the efficiency of organic carbon transfer out of the surface ocean (Suttle, 2007; Brussaard *et al*., 2008a).

As in many other marine environments, the virioplankton in the waters surrounding Antarctica have been shown to be an active component of the ecosystem (Guixa-Boixereu *et al*., 2002; Pearce *et al*., 2007; Thomson *et al*., 2010; Evans and Brussaard, 2012; Brum et al., 2016). Nevertheless, they are omitted from most current models of the Southern Ocean food web (e.g., Murphy *et al*., 2013) due to a lack of knowledge of the way virioplankton respond to the extreme seasonality in polar waters, and more importantly the pronounced year-to-year variations in the productivity of these systems. Intense seasonal phytoplankton blooms that are controlled by marked variations in irradiance and sea ice dynamics form the base of the productive Antarctic marine ecosystem (Ducklow *et al*., 2007; Clarke *et al*., 2007; 2008). In turn, fluctuations in phytoplankton abundance and primary productivity are thought to control the activity and dynamics of the bacterioplankton community via the supply of photosynthate (Ducklow *et al*., 2012). Differences in the observed levels of coupling between primary and secondary production in polar ecosystems have led to the suggestion that photosynthate may have variable bioavailability (Moran *et al*., 2002; Bird and Karl, 1999), or that top-down control might have greater significance in controlling bacterioplankton dynamics (Ortega-Retuerta *et al*., 2008). Alternatively, the release of organic carbon by phage lysis of bacterial cells has been suggested as a substrate source for

bacterioplankton in Antarctic waters, which could weaken the link between primary and secondary producers (Evans and Brussaard, 2012).

The Western Antarctic Peninsula (WAP) is an important focus of research activity, due to the fact that during the instrumental period it has been one of the most rapidly warming regions on Earth (Smith *et al*., 1996; Vaughan *et al*., 2003; Meredith and King, 2005). The rapid warming has recently been observed to have paused (Turner et al. 2016), and the trajectory/timing of future climate change is not clear. Nonetheless, a warming due to the influence of increasing atmospheric greenhouse gases is expected, and a mechanistic understanding of WAP marine processes is required in order to obtain insight into the potential impacts of that warming. The regional effects of climate change have been observed at various trophic levels of the food web, from shifts in the composition of phytoplankton assemblages (Moline *et al*., 2004; Montes-Hugo *et al*., 2009) through to reductions in the numbers of Adélie Penguins (*Pygoscelis adeliae*; Fraser and Trivelpiece, 1995). Because of their short generation times and free-floating planktonic lifestyles, microbes are expected to react rapidly to environmental conditions (Hays *et al*., 2005), and their sensitivity to projected changes in polar systems has been highlighted (Kirchman *et al*., 2009; Ducklow *et al*., 2010).

Eulerian, multi-year time series are a powerful tool with which to dissect the web of factors controlling functional microbial groups in marine systems, thereby helping to identify the potential implications of ongoing climate change. This approach has been successfully applied to unraveling the mechanisms controlling bacterioplankton and phytoplankton dynamics adjacent to the WAP (Clarke *et al*., 2007; Ducklow *et al*., 2012; Venables *et al*., 2013). The importance of this endeavor to marine virus ecology has been highlighted (Breitbart, 2012), and multi-year time series have improved our understanding of the virioplankton from open ocean and coastal environments (Parsons *et al*., 2012; Pagarete *et al*., 2013; Hurwitz et al., 2014). However, the interannual dynamics of the virioplankton prevalent in polar coastal waters, and their driving forces are as yet undetermined. Here we present an eight-year virioplankton

Wiley-Blackwell and Society for Applied Microbiology

dataset with unprecedented temporal resolution from a climatically-sensitive WAP site (Fig. 1). Our aims are to establish: (1) the seasonal and inter-annual dynamics of virioplankton; (2) what linkages exist between the physiochemical and biological parameters, with a view to unravel the factors driving virus dynamics, and how viruses might in turn influence ecosystem function; (3) a baseline against which future virus data might be compared; and finally (4) how future changes associated with predicted greenhouse-gas driven warming at the WAP might impact on the virioplankton, and in turn affect ecosystem functioning.

Results

Study site and physicochemical setting

All data for this study were collected off the Western Antarctic Peninsula at the Rothera Oceanographic and Biological Time Series (RaTS) sampling sites #1 (67.570ºS 68.225ºW) and occasionally #2 (67.581ºS 68.156ºW), both situated in Ryder Bay, Adelaide Island (Fig. 1).

[insert figure 1 - map]

Weekly averages of the environmental conditions during the 8-year sampling period are presented in the composite plots shown in Figure 2, while more detailed time series plots of individual parameters to showcase inter-annual variations are shown in Figure 3. The strong seasonality in the physiochemical conditions at the RaTS site is due to its high latitude location (see additional discussion in the Supplementary Materials). A substantial ice cover (pancake or pack ice, with fast ice developing during most years), low water temperatures of -1.7±0.1°C, salinity levels of 33.7±0.2 and a deep but variable mixed layer at 65±30 m are characteristic of winter conditions which commence between April and June. Summer conditions return between early October and early January: the sea ice cover rapidly decreases (to brash or ice-free) and a stratified water column develops with a mixed layer depth of less than 20 m and water temperatures of up to 1.8°C (median 0.7°C). Nutrient concentrations are highest

during winter and decrease during the phytoplankton spring bloom, although this decrease is much less pronounced for silicate than it is for phosphorous and NOx.

[insert figure 2 – physicochemical averages]

It should be noted that the situation described here is an average over the observed 8 year time period, and that significant inter-annual variations exist in the timing and magnitude of these changes (Fig. 3). For example, in the winter of 2005 fast ice conditions prevailed from mid-May until the turn of the year, whereas the winter of 2007 was characterized by mostly ice-free conditions, and significant sea ice cover during the winter of 2008 only lasted for two months.

[insert figure 3_part 1 – physicochemical full time series]

[insert figure 3_part 2 – physicochemical full time series]

Dynamics of phytoplankton, bacteria and viruses

Phytoplankton, as determined by chlorophyll *a* concentrations, are virtually absent throughout the winter period. With the disappearance of sea ice in spring phytoplankton biomass increases sharply (median onset in the first week of November; Fig. 4A). During the sequence of summers from 2002-2007 chlorophyll *a* concentrations reached maxima of up to 27 µg L^{-1}, while for the remaining four summers the maxima were substantially lower at 8-18 µg L^{-1} (Fig. 5A). Each year the phytoplankton bloom declines sharply to low levels (<1 mg m^{-3}) at the end of summer (median during the first week of April), and continues to slowly decrease to winter concentrations throughout the autumn.

[insert figure 4 – biology averages]

As with the primary producers, the bacterioplankton (bacterial and archaeal cells) show a strong seasonal cycle in most years. Bacterioplankton numbers start to increase from winter minima of 2.0±0.8 x 10^8 cells L^{-1} around the same time as the phytoplankton, albeit not as rapidly and not reaching maximum values until 2-3 weeks later (Fig. 4B; lags were calculated from average number of days

between first maxima of the spring bloom, as well as subsequent maxima later on in the season). These maxima vary strongly from year to year, being low in the summers of 2003-2005 (about 0.5 x 10^9 cells L^{-1}), consistently high throughout the summers of 2005-2007 (about 2.0 x 10^9 cells L^{-1}), and fairly high but more variable in the remaining summers (average 1.5 x 10^9 cells L^{-1}) (Fig. 5B). Bacterioplankton numbers decline later and much less sharply than the phytoplankton, and generally do not reach winter values until June. The bacterioplankton community was subdivided into cells with high and low DNA content (HNA and LNA, respectively) according to their green fluorescence after staining with SYBR Green (Gasol *et al*., 1999). The HNA subgroup is on average more abundant throughout the year than the LNA subgroup, constituting around 70% of total bacterioplankton in spring and summer, and between 50 and 60% during winter (Fig. 4D). However, in some years the LNA subgroup was more abundant, particularly pre-2007 (Fig. 5C).

Virioplankton abundances closely track the bacterioplankton with a lag of about a week (Fig. 4C), although this is less pronounced in years with low prokaryote and viral numbers. Maximum virioplankton numbers reach values of 1-2 x 10^{10} particles L^{-1} in most years, but were double that in the summers of 2005-2007 (up to 4.5 x 10^{10} particles L^{-1}) (Fig. 5E). In addition, during the summer of 2009-2010 a brief spike in virus numbers (4.8 x 10^{10} particles L^{-1}) occurred at the start of March. Like the bacterioplankton, virioplankton numbers do not decrease sharply at the end of the bloom period, but rather decrease gradually throughout the autumn and most of the winter. As a result, winter virioplankton numbers are quite variable and reflect the size of the preceding summer bloom. For example during the winter of 2006 virus numbers were twice as high as in other winters, following on from the high virioplankton abundances in the summer of 2005/2006. Three distinct virus subgroups were distinguished by flow cytometry based on the green fluorescence signal of their stained nucleic acids (Supplementary Materials, Figure S2), in accordance with previous results from the Southern Ocean (Brussaard *et al*., 2008b; Evans *et al*., 2009). Viral subgroup V1 (lowest fluorescence) is generally

the most abundant group (26-93%), followed by V2 (6-60%) and V3 (highest fluorescence; 1-14%) (Fig. 4E). Although the magnitudes of change between summer and winter, as well as between different years, are similar for all three viral groups, the dynamics of V1 are somewhat different from those of V2 and V3 (Fig. 5F-H). During summer the virioplankton community is dominated by V1, but during most winters the relative abundances of V2 and V3 increase to equal that of V1 (Fig. 4E), although this is not the case in every year.

The virus-to-bacteria ratio (VBR) is generally around 20-30, although in some years it increases up to ~90 during summer and coinciding with the increases in bacterio- and virioplankton numbers (Fig. 5D).

[insert figure 5_part 1 – biology full time series]

[insert figure 5_part 2 – biology full time series]

Inter-annual variation in plankton dynamics and correlation with environmental data

Multivariate analysis was performed to determine trends in the inter-annual variation in the planktonic abundances and community composition, and to find the environmental drivers behind these dynamics. As detailed in the Experimental Procedures, the time series was split into 16 seasonal segments (summer/winter) and the integrated values for each segment were used for statistical analyses. Principal coordinates ordination (PCO) of the biological data shows that 87.8% of its variation can be accounted for by two axes, which represent the seasonal and year-to-year differences at the site (Fig. 6). The strong seasonal pattern in chlorophyll concentrations and bacterio- and virioplankton abundances (low in winter and high in summer accounts) already explains 72.5% of the variation. This pattern is confirmed by the vector plot overlays, and yields two significantly different clusters (i.e., summer and winter) along the horizontal axis (ANOSIM test: $p<0.01$, 9999 permutations). The vertical axis explains a further 15.3% of the variation and represents year-to-year differences in the composition of the plankton community, driving the abundances of viral group V1 and HNA bacteria on the one hand, and

phytoplankton and viral group V3 on the other, with viral group V2 and LNA bacteria being intermediate.

[insert figure 6 - PCO]

In order to identify which environmental parameters could be driving these dynamics at the WAP the biological clustering results were first correlated with the available physicochemical data (vector plot in Fig. 6). As expected, temperature and ice cover correlate with the seasonal trend (PCO axis 1), as does phosphate. The factors that also correlate with the secondary PCO axis are silicate and NOx (both positive), salinity and MLD (both negative). Distance-based linear models (distLM) were used to further interrogate these results. Forward selection in combination with the Akaike Information Criterion (AIC) criteria selected salinity, phosphate, silicate and to a lesser extent NOx as the most influential variables. A distLM comprising these four variables was able to explain nearly 70% of the total variation in the biological community (Fig. 7).

[insert figure 7 – distLM model]

Discussion

Drivers of virioplankton at the WAP

Virioplankton abundances at the coastal WAP showed a pronounced seasonal cycle with interannual variability in the timing and magnitude of the summer maxima. Viral abundances are primarily linked to the type and availability of their microbial hosts, although they may also be influenced directly by shifts in environmental conditions (Mojica and Brussaard, 2014). As the numerically dominant hosts, bacterioplankton abundance was the most influential factor in virioplankton dynamics (Weinbauer, 2004), with shifts in the former generally mirrored by the latter following a lag of approximately one week. Bacterioplankton production in coastal Antarctic waters is regulated indirectly by the levels of phytoplankton biomass accumulation and rates of primary production, as this determines substrate

availability (Ducklow *et al*., 2012). In turn, the temporal variability of primary production, and thus phytoplankton biomass, at high latitudes is constrained by sea ice cover and seasonal duration during winter. This in turn influences the timing and magnitude of the spring-summer blooms, the stability of the water column, and the availability of light and iron (Vernet *et al*., 2008; Venables *et al*., 2013 Saba *et al*., (2014)). Consequently, one would expect to see a strong relationship between chlorophyll, bacterioplankton and in turn viral dynamics, driven primarily by the sea ice conditions of the preceding winter and subsequent summer mixing. Our data revealed that the coupling of bacterioplankton and virioplankton to chlorophyll is variable, with the magnitude of the chlorophyll for a given year not necessarily predicting the magnitude of bacterioplankton yield for that same year. Thus, factors other than those which determine phytoplankton accumulation are implicated as indirect drivers of virioplankton via their influence on bacterioplankton and these are discussed below.

Decoupling between primary and secondary production in the coastal Antarctic has been previously reported (Bird and Karl, 1999; Moran *et al*., 2001; Duarte *et al*., 2005), although as the time series confirms, it is not the general state for this ecosystem (Ortega-Retuerta *et al*., 2008; Ducklow *et al*., 2012). Low temperature preclusion of optimal substrate assimilation has been proposed as an explanation for low microbial rates, and thereby decoupling, in high latitude ecosystems (Pomeroy and Wiebe, 2001), but we found temperature not to be a significant driver of the microbial system. Instead, its variability appears to relate to levels of the macronutrients NOx, phosphate and silicate. In coastal Antarctic waters, macronutrients are considered to be replete; however drawdown to potentially limiting levels can occur during periods of high primary productivity (Ducklow *et al*., 2007; Alderkamp *et al*., 2012). It is interesting to note that whilst levels of dissolved inorganic nitrogen and phosphorous strongly co-varied, silicate levels were more distinct (Figs 3 and 6). The level and stoichiometry of nutrient drawdown is controlled by the productivity and composition of the phytoplankton community, which in coastal Antarctic waters varies annually and is made up primarily of diatoms and small

Wiley-Blackwell and Society for Applied Microbiology

flagellated cells, particularly the Prymnesiophyte *Phaeocystis antarctica* (Garibotti *et al*., 2005; Clarke *et al*., 2008; Annett *et al*., 2010). The distinction in silicate's influence from that of the other macronutrients could indicate that the phytoplankton composition, i.e. the relative contribution of diatoms (Kim *et al*., 2016), affects bacterioplankton dynamics, and thereby indirectly the virioplankton. This influence is most likely mediated by variations in the quantity and/or bioavailability of organic matter generated by the primary producers, which is proposed to vary according to phytoplankton taxa (Moline and Prezelin, 1996), and may affect bacterioplankton biomass (Ducklow et al., 2012) and composition (Tada *et al*., 2013). Indeed, the bioavailability of photosynthate to secondary producers has been proposed as an alternative explanation for the decoupling of primary and secondary producers in Antarctic waters (Fiala and Delille, 1992). Drawdown of macronutrients by phytoplankton requires iron to be available, and interannual variation in summer macronutrient minima could be indicative of variable iron supply from melting glaciers (Gerringa *et al*., 2012). Iron is known to be a limiting factor to Southern Ocean bacterioplankton communities (Church *et al*., 2000), and variations in its availability may exert indirect influence over virioplankton dynamics.

Throughout the seasonal cycle, the highest VBR values were observed in the summer, most likely as a result of higher burst sizes (yield of viruses per host cell lysed) and rates of virally-mediated mortality in the productive summer months (Brum *et al*., 2016). Maximal substrate inputs by primary producers during the summer months stimulates metabolic activity in bacterioplankton (Ducklow *et al*., 2012), a parameter predictive of burst size (Lenski, 1988; Weinbauer and Holfe, 1998; Middelboe, 2000). Bacterioplankton diversity is also known to decrease from winter to summer (Ghiglione and Murray, 2012; Grzymski *et al*., 2012), which will increase the likelihood of successful infection in the summer (Murray and Jackson, 1992; Weinbauer and Holfe, 1998). Hence, water column stability reduces bacterioplankton diversity and in turn, enhances viral production rates (Winget *et al*., 2011); thereby explaining the lower viral yields observed in the deeply mixed years of the time-series (2008-2011).

Furthermore, lower host abundances in winter promote a shift towards lysogenic over lytic viral infection (Brum *et al*., 2016), reducing levels of viral production and VBR, as has been shown for the Southern Ocean (Evans and Brussaard, 2012).

Tight control of bacterioplankton by top-down factors has been suggested as an alternative explanation for the lack of coupling between primary and secondary production in coastal Antarctic waters (Ortega-Retuerta *et al*., 2008). Typically, top-down control is thought to be mediated by grazers (Bird and Karl, 1999; Duarte *et al*., 2005), although viruses have also been suggested to fulfill this role (Guixa-Boixereu *et al*., 2002). Indeed high levels of phage activity are indicated by the close coupling of the bacterio- and virioplankton dynamics throughout the RaTS time series (Figs 4, 5 and 6) and supported by reports of virus-mediated mortality in the waters surrounding Antarctica (Guixa-Boixereu *et al*., 2002, Evans and Brussaard, 2012; Brum *et al*., 2016). Furthermore, as lysates (the hosts cellular contents released during viral lysis) serve as bacterial substrates (Middelboe *et al*., 1996; Wilhelm and Suttle, 1999; Suttle, 2007) high levels of viral infection may reduce bacterioplankton's reliance upon phytoplankton derived substrates. This may further serve to decouple primary and secondary production in the waters around Antarctica (Evans and Brussaard, 2012).

Composition of the viral community

The V1-V3 virus groups all accumulate and decline in line with the wax and wane of primary and secondary producers (Figs. 4 and 5), although their dynamics, particularly those of V1 and V3, appear to be independent of one another (Fig. 5G-H) and their relative contribution to the total viral assemblage varies from year to year. V1 is the most abundant, closely following the dynamics of the bacterioplankton (HNA and LNA), whereas V3 partitions more closely with chlorophyll (Fig. 6). Marine viral assemblages are diverse, but are presumably dominated by those viruses pathogenic to the most abundant microbial hosts (Angly *et al*., 2006). Our results align with previous findings from polar oceans that suggest the numerically dominant, low fluorescence group V1 is most likely to

contain bacteriophages, whereas the higher fluorescent V2 and V3 groups are thought to be viruses of phytoplankton (Payet and Suttle, 2007; Brussaard *et al*., 2008b; Evans *et al*., 2011). During the three summers where bacterioplankton reached their highest levels (2005-2006, 2006-2007 and 2009-2010 [Fig. 5B]), VBR was highest when compared to the remaining years (Fig. 5D), and V1 appeared to make up a far greater proportion of the total viral assemblage (Figs 5F-H), supporting the hypothesis that V1 may be bacteriophages. Interestingly, during the summer months when bacterioplankton exhibited lowest abundances (summers 2003-2004), V1's contribution to the total virioplankton was also at a minimum. In addition, the VBR was at its highest, suggesting that virus production was from other (eukaryotic) sources. This variability in the availability of potential microbial hosts directly influenced both the abundance and composition of the virioplankton in the coastal WAP waters.

Viral control of microbial populations

Multivariate statistical analysis revealed stronger association of the V1 group with the HNA compared to the LNA, consistent with reports that suggest viral infection of HNA results in larger burst sizes than LNA, and likely accounts for the majority of viral production (Payet and Suttle, 2008; Bouvier and Maurice, 2011). HNA have been proposed to have a higher metabolic activity relative to LNA (Lebaron *et al*., 2001), although this is not always the case (Zubkov *et al*., 2001; Longnecker *et al*., 2005). Differences between the two categories have been attributed to their growth states, as studies indicate they are not always phylogenetically distinct (Lebaron *et al*., 2002, Longnecker *et al*., 2005). Yet, Zubkov and coworkers (2001) found that flow cytometric subgroups of prokaryotes were affiliated with different phylogenetic clusters.

Throughout the time series we saw a seasonal shift in the relative abundance of the two bacterioplankton groups: while they were more or less equally abundant in winter, HNA dominated

during summer, at times comprising >90% of bacterioplankton (Fig. 5C). This result could be consistent with the idea that HNA are more metabolically active, as they appear to dominate in the months when more substrates would be available via either primary producers, or mortality of secondary producers. However, along the Antarctic Peninsula LNA cells have been shown to relate more closely to secondary production than HNA, indicating nucleic acid content is an unreliable proxy for metabolic activity (Ortega-Retuerta *et al*., 2008). Thus, it seems more likely that the seasonal shifts in H/LNA ratio reflect changes in the composition of the bacterioplankton community. Metagenomic assessment of the prokaryotes from the WAP supports this theory, as community composition differs from summer to winter (Grzymski *et al*., 2012). Hence, the weaker relationship between V1 and LNA relative to HNA could be interpreted to indicate that bacterioplankton clades with smaller genomes were subject to less viral infection than those with larger genomes. While we do not have molecular identification of the bacterioplankton groups, we speculate that the primary phylotype of the LNA group may belong to the SAR11 clade since it is identified as a dominant component of the bacterioplankton assemblage at the WAP (Grzymski *et al*., 2012), is characterized by a small genome (Giovannoni *et al*., 2005) and has been shown to make up the vast majority of LNA in marine waters (Gómez-Pereira *et al*., 2013). SAR11 has been proposed to be a defense specialist, allowing it to co-exist with its phage and maintain its abundance (Suttle, 2007; Zhao *et al*., 2013), and evidence from a time series in the Sargasso Sea suggests its viruses comprise a disproportionally small percentage of the total virioplankton (Parsons *et al*., 2012). Our results would then support the hypothesis that viral infection rates of this clade are low. In this case the weaker correlation between V1 and LNA (Fig. 6) may be more indicative of a co-dependency of both on HNA, as a host for the former and potentially as substrate source for the latter. Alternatively, the greater abundance of HNA relative to LNA potentially masked viral production from the latter, a phenomenon that would be compounded by lower burst sizes (Bouvier and Maurice, 2011).

Conversely a tight control of HNA by viruses, and particularly V1, is apparent from their pronounced co-variation, the most striking example of which occurred during February to March 2010. A spike in HNA abundance was observed in concert with a spike in V1 abundance (offset by approximately one week), indicative of a viral-induced bacterioplankton bloom crash (Fig. 8). Oscillations such as these could be interpreted as the rapid multiplication of a specific host strain, followed by the proliferation of a virus pathogenic to that strain by infection and death of the host, making the niche available to resistant strains. This model of predator-prey interactions has been proposed as a theory which explains the diversity in microbial communities and is termed the 'Kill the Winner' hypothesis (Thingstad and Lignell, 1997; Thingstad, 2000). By inference, the HNA is likely composed of a diverse bacterioplankton assemblage, containing some or all competition strategists (Suttle, 2007), and whose dominance is variable and determined, at least in part, by viruses. Interestingly, though perhaps unsurprisingly, viral and prokaryote communities' coexistence appeared more stable throughout the winter months when bacterioplankton diversity (Grzymski *et al*., 2012), and thus host diversity is greater. However, as the Kill the Winner model of virus-host dynamics has also been linked to the maintenance of susceptible hosts at lower levels of abundance (Bouvier and del Giorgio, 2007), it is plausible that under the less dynamic conditions of winter, viruses aid in maintaining bacterioplankton diversity.

[insert figure 8 – HNA and V1 Feb-Mar 2010]

Outlook: virioplankton at the WAP in a changing climate

Understanding the dynamic aspects of ocean microbial communities in response to seasonal processes can inform predictions of their response and resilience to environmental perturbation (Giovannoni and Vergin, 2012). Our findings imply linkages between the physiochemical conditions and virioplankton activity, mediated by effects on the functioning of the microbial food web. Interestingly, viral activity, as mediated by bacterioplankton dynamics and likely also diversity, was not directly coupled to

phytoplankton biomass. Instead, our results are suggestive of the influence of phytoplankton assemblage composition, as indicated by differences in inter-annual nutrient stoichiometery. The long-term warming along the WAP (which has recently weakened however [Turner *et al*., 2016]) is causing a shift from a maritime-Antarctic climate to a warmer sub-Antarctic-type climate. The resultant reductions in sea ice extent, concentration (e.g., Holland, 2014) and seasonal duration (Stammerjohn *et al*., 2012) have implications on the composition of phytoplankton assemblages (Moline *et al*., 2004; Montes-Hugo *et al*., 2009), as well as reductions in the magnitude of phytoplankton blooms (Venables *et al*., 2013). Phytoplankton species are predicted to shift from large diatoms to smaller forms (Falkowski and Oliver, 2007) with consequences for the structure and activity of Antarctic bacterioplankton assemblages (Ghiglione and Murray, 2012), likely mediated by the supply of bacterial substrates (Kirchman *et al*., 2009). Our findings suggest these shifts will have implications for the activity and degree of virioplankton influence. This will have consequences for the flow of matter and energy through the viral shunt and their availability to the Antarctic food web (Suttle, 2005), as well as the cycling of elements such as iron and carbon (Poorvin *et al*.,2004; Evans *et al*., 2009). For example, viral infection has been proposed to either reduce the efficiency of the biological pump by converting particulate to dissolved organic matter, or to promote carbon sinking by stimulating particle aggregation (Brussaard *et al*., 2008a). Thus, future shifts in viral activity may influence the WAP's ability to act as a CO_2 sink. Viruses are dynamic and active components of the coastal waters of the WAP and wider marine Antarctic environment and we recommend their inclusion in models of Antarctic ecosystem functioning. Given the apparent sensitivity of viral activity to potential future changes at the WAP (a region noted already for strong climatic sensitivity), further study is warranted to quantify viral-mediated mortality and determine its role in element cycling and the functioning of the Antarctic food web. Furthermore, our study highlights the need for future work to assign identities to the main players within the viral and

microbial communities studied, and in particular to confirm that SAR11 is the dominant component of the LNA at the WAP, in order to better understand their ecological and biogeochemical role.

Experimental Procedures

Study site and sampling

The Rothera Oceanographic and Biological Time Series (RaTS) sampling site is situated at the south-eastern point of Adelaide Island, adjacent to the Western Antarctic Peninsula (WAP; Fig. 1). The primary RaTS site (Site 1) is located at 67.570ºS 68.225ºW in Ryder Bay, approximately 4 km from the British Antarctic Survey's Rothera Research Station, and has a water depth of 520 m. At times when (partial) sea ice cover precludes access to Site 1 by either boat or skidoo, sampling is performed at RaTS site 2, which is located at 67.581ºS 68.156ºW and has a water depth of 300 m. The two sites exhibit no significant difference in seasonal cycle or water column characteristics and are therefore considered equivalent (Clarke *et al*., 2008). Sampling for microbial abundances commenced in January 2003 and has continued approximately twice weekly in austral summer (hence forward referred to as summer) and approximately twice monthly in austral winter (hence forward referred to as winter), although no data are available from March 2007 to March 2008 owing to loss of the samples collected during this period. Discrete water sampling at a depth of 15 m was performed for samples of viruses, prokaryotes and nutrients, using a Niskin bottle deployed by winch from either a rigid inflatable boat or a sledge. Vertical profiles of water column salinity, temperature, density and chlorophyll concentration were obtained using a SeaBird 19+ instrument and a WetLabs in-line fluorometer (see Clarke *et al*., 2008 for full details).

Bacterio- and virioplankton abundances

For enumeration of viruses and bacteria, 2 mL seawater samples were fixed with a final concentration of 0.5% glutaraldehyde (EM grade, Sigma Aldrich, USA) and stored at -80ºC. Viral and prokaryote

abundances were determined according to the methods of Mojica *et al*. (2014) and Marie *et al*. (1999), respectively. Briefly, samples were defrosted immediately prior to analysis, diluted with TE-buffer (pH 8.2) and stained with SYBR-Green I (Molecular Probes, Invitrogen, USA) at a final concentration of 0.5 x 10^{-4} (viruses) and 1 x 10^{-4} (bacteria) of the commercial stock. Staining was completed in the dark for 10 min at 80ºC for viral samples, and at room temperature for 15 min for bacterioplankton samples. Counts were performed on a Becton-Dickinson FACSCalibur flow cytometer (BD Biosciences, USA). Groups were determined in bivariate scatter plots of green fluorescence of stained nucleic acids versus side scatter.

Data analysis

All data analyses were performed in parallel in the dedicated software package PRIMER 6 (PRIMER-E, Lutton; Clarke and Gorley, 2006; Anderson *et al*., 2008) and the *R* package VEGAN (Dixon, 2003; Oksanen *et al*., 2013). Our aims were first to describe the interannual variability in abundances of bacterio-, virio- and phytoplankton (expressed as chlorophyll levels), and second to determine which physicochemical parameters are driving this variability. To reduce noise levels in the high resolution data and omit the problems associated with missing data, integrated values (area under curve) were calculated for each variable. Furthermore, to facilitate year-by-year comparison of the biological variability, the time series was subdivided into “summer” and “winter” time segments, using the level of local sea ice cover in Ryder Bay (visual assessment) and in the wider Marguerite Bay area (satellite data; Stammerjohn *et al*. 2008; 2012) as an independent criterion (see Supplementary Material a full discussion).

To visualize the similarity between the different summer and winter time segments, PCO plots were constructed on the biological data using the Euclidian distance of square root transformed and normalized values (the PCO of a Euclidian distance-based matrix is equivalent to a Principal Component Analysis). Biological variables included the virioplankton groups V1, V2 and V3, HNA and LNA bacterioplankton, and chlorophyll as representative of phytoplankton abundance. Correlations between

Wiley-Blackwell and Society for Applied Microbiology

the biological and physicochemical data and the PCO axes are illustrated with a vector plot (Pearson product-moment correlation coefficient). The direction of each vector reflects the direction of increase of the variable (i.e., higher number or magnitude), whereas the vector length represents the strength of the correlation (i.e., between the variable and the distribution of the biological data). To model which of the measured physicochemical variables are able to explain the interannual variance in the biological dataset we performed a redundancy analysis. A distance-based linear mixed model (DistLM in PRIMER) was constructed which used a combination of the Akaike Information Criterion (AIC) and a forward selection procedure to select the most significant and useful predictor variables. The DistLM results are visualized here with dbRDA (distance-based redundancy analysis) plots. The PRIMER results were confirmed by performing a separate redundancy analysis on the same data in the *R* package VEGAN, which yielded comparable outcomes.

Acknowledgments

This work was supported by the Division for Earth and Life Sciences (ALW) with financial input from the Netherlands Organization for Scientific Research (NWO) under grant number 851.20.047. We gratefully acknowledge the British Antarctic Survey's Rothera Research Station Marine Assistants who collected samples and CTD data during the study period, namely Andrew Miller, Paul Mann, Helen Rosetti, Alison Massey, Terri Souster and Simon Reeves. We would also like to thank Peter-Paul Stehouwer and Cees van Slooten for their assistance with the virus counts.

References

Alderkamp, A.-C., Mills, M.M., van Dijken, G.L., Laan, P., Thuróczy, C-E., Gerringa, L.J.A., *et al*. (2012) Iron from melting glaciers fuels phytoplankton blooms in the Amundsen Sea (Southern Ocean): Phytoplankton characteristics and productivity*. Deep Sea Res Part II* 71–76: 32–48.

Anderson, M.J., Gorley, R.N., and Clarke, K.R. (2008) PERMANOVA+ for PRIMER: Guide to software and statistical methods. PRIMER-E, Plymouth.

Angly, F.E., Felts, B., Breitbart, M., Salamon, P., Edwards, R.A., Carlson, C., *et al*. (2006) The marine viromes of four oceanic regions. *PLoS Biol* 4: 2121-2131.

Annett, A.L., Carson, D.S., Crosta, X., Clarke, A., and Ganeshram, R.S. (2010) Seasonal progression of diatom assemblages in surface waters of Ryder Bay Antarctica. *Polar Biol* 33:13-29.

Bird, D.F., and Karl. D.M. (1999) Uncoupling of bacteria and phytoplankton during the austral spring bloom in Gerlache Strait, Antarctic Peninsula. *Aquat Microb Ecol* 19: 13-27.

Bouvier, T., and del Giorgio, P.A. (2007) Key role of selective viral-induced mortality in determining marine bacterial community composition. *Environ Microbiol* 9: 287-97.

Bouvier, T., and Maurice, C.F. (2011) A single-cell analysis of virioplankton adsorption, infection, and intracellular abundance in different bacterioplankton physiologic categories. *Microb Ecol* 62: 669-678.

Breitbart, M. (2012) Marine viruses: truth or dare. *Ann Rev Mar Sci* 4: 425-48.

Brum, J.R., Hurwitz, B.L., Schofield, O., Ducklow, H.W., Sullivan, M.B. (2016) Seasonal time bombs: dominant temperate viruses affect Southern Ocean microbial dynamics. *ISME J* 10: 437-449.

Brussaard, C.P.D., Timmermans, K.R., Uitz, J., and Veldhuis, M.J.W. (2008b). Virioplankton dynamics and virally induced phytoplankton lysis versus microzooplankton grazing southeast of the Kerguelen (Southern Ocean). *Deep Sea Res Part II* 55: 752-765.

Brussaard, C.P.D., Wilhelm, S.W., Thingstad, F., Weinbauer, M.G., Bratbak, G., Heldal, M., *et al.* (2008a) Global-scale processes with a nanoscale drive: the role of marine viruses. *ISME J* 2: 575-578.

Church, M.J., Hutchins, D.A., and Ducklow, H.W. (2000) Limitation of bacterial growth by dissolved organic matter and iron in the Southern Ocean. *Appl Environ Microbiol* 66: 455-466.

Clarke, A., Meredith, M.P., Wallace, M.I., Brandon, M.A., and Thomas, D.N. (2008) Seasonal and interannual variability in temperature, chlorophyll and macronutrients in northern Marguerite Bay, Antarctica. *Deep Sea Res Part II* 55: 18–19.

Clarke, A., Murphy, E.J., Meredith, M.P., King, J.C., Peck, L.S., Barnes, D.K.A., and Smith R.C. (2007) Climate change and the marine ecosystem of the western Antarctic Peninsula. *Philos Trans R Soc Lond B Biol Sci* 362: 149-166.

Clarke, K.R., and Gorley, R.N. (2006) PRIMER v6: User manual/tutorial. PRIMER-E, Plymouth.Dinsdale, E.A., Edwards, R.A., Hall, D., Angly, F., Breitbart, M., Brulc, J.M., *et al*. (2008) Functional metagenomic profiling of nine biomes. *Nature* 452: 629–33.

Dixon, P. (2003) VEGAN, a package of R functions for community ecology. *J Veg Sci* 14: 927-930.

Duarte. C.M., Agusti, S., Vaque, D., Agawin, N.S.R., Felipe, J., Casamayor, E.O., Gasol, J.M. (2005) Experimental test of bacteria–phytoplankton coupling in the Southern Ocean. *Limnol Oceanogr* 50: 1844-1854.

Ducklow, H.W., Baker, K., Martinson, D.G., Quetin, L.B., Ross, R.M., Smith, R. M., *et al*. (2007) Marine pelagic systems: the West Antarctic Peninsula. *Phil Trans R S B* 362: 67–94.

Ducklow, H.W., Morán, X.G., and Murray, A.E. (2010) Bacteria in the Greenhouse: Marine Microbes and Climate Change. In Mitchell, R., Gu, J.D. Environmental Microbiology, 2nd edn. Wiley-Blackwell, Hoboken, NJ, p 363.

Ducklow, H.W., Schofield, O., Vernet, M., Stammerjohn, S., and Erickson, M. (2012) Multiscale control of bacterial production by phytoplankton dynamics and sea ice along the western Antarctic Peninsula: A regional and decadal investigation. *J Mar Syst* 98–99: 26–39.

Evans, C., and Brussaard, C.P. (2012) Regional variation in lytic and lysogenic viral infection in the Southern Ocean and its contribution to biogeochemical cycling. *Appl Environ Microbiol*. 78: 6741-6748.

Evans, C., Pearce, I., and Brussaard, C.P.D. (2009) Viral mediated lysis of microbes and carbon release in the sub-Antarctic and Polar Frontal Zones of the Australian Southern Ocean. *Environ Microbiol* 11: 2924-2934.

Evans, C., Thomson, P.G., Davidson, A.T., Bowie, A.R., van den Enden, R., Witte, H., and Brussaard, C.P.D. (2011) Potential climate change impacts on microbial distribution and carbon cycling in the Australian Southern Ocean. *Deep Sea Res Part II* 58: 2150-2161.

Falkowski, P.G., and Oliver, M.J. (2007) Mix and match: how climate selects phytoplankton. *Nat Rev Microbiol* 5: 813-819.

Fiala, M., and Delille, D. (1992) Variability and interactions of phytoplankton and bacterioplankton in the Antarctic neritic area. *Mar Ecol Prog Ser* 89:135-146.

Fraser, W.R., and Trivelpiece, W.Z. (1995) Palmer LTER: relationships between variability in sea-ice coverage, krill recruitment and the foraging ecology of Adelie Penguins. *Ant J U S* 30: 271-272.

Garibotti, I.A., Vernet, M., and Ferrario, M.E. (2005) Annually recurrent phytoplanktonic assemblages during summer in the seasonal ice zone west of the Atarctic Peninsula (Southern Ocean). *Deep Sea Res I* 52: 1823-1841.

Gasol, J.M., Zweifel, U.L., Peters, F.C., Fuhrman, J.A., and Hagstrom, A. (1999) Significance of size and nucleic acid content heterogeneity as measured by flow cytometry in natural planktonic bacteria. *Appl Environ Microbiol*. 65: 4475-4483.

Gerringa, L.J.A., Alderkamp, A.-C., Laan, P., Thuróczy, C.-E., De Baar, H.J.W., Mills, M.M., *et al*. (2012) Iron from melting glaciers fuels the phytoplankton blooms in Amundsen Sea (Southern Ocean); iron biogeochemistry. *Deep Sea Res II* 71–76:16–31.

Ghiglione, J.F., and Murray, A.E. (2012) Pronounced summer to winter differences and higher wintertime richness in coastal Antarctic marine bacterioplankton. *Environ Microbiol* 1 4:617-29.

Giovannoni, S.J., Tripp, H.J., Givan, S., Podar, M., Vergin, K.L., Baptista, D., *et al*. (2005) Genome Streamlining in a Cosmopolitan Oceanic Bacterium. *Science* 309: 1242-1245.

Giovannoni, S.J., and Vergin, K.L. (2012) Seasonality in ocean microbial communities. *Science* 335: 671-676.

Gomez-Pereira, P.R., Hartmann, M. Grob C., Tarran G.A., Martin A.P., Fuchs B.M., Scanlan D.J., Zubkov, M.V. (2013) Comparable light stimulation of organic nutrient uptake by SAR11 and *Prochlorococcus* in the North Atlantic subtropical gyre. *ISME J* 7:603-614.

Grzymski, J.J., Riesenfeld, C.S., Williams, T.J., Dussaq, A.M., Ducklow, H., Erickson, M., *et al*. (2012) A metagenomic assessment of winter and summer bacterioplankton from Antarctica Peninsula coastal surface waters. *ISME J* 6: 1901-1915.

Guixa-Boixereu, N., Vaqué, D., Gasol, J.M., Sánchez-Cámara, J., and Pedrós-Alió, C. (2002) Viral distribution and activity in Antarctic waters. *Deep Sea Res Part II* 49: 827-845.

Hays, G.C., Richardson, A.J., and Robinson, C. (2005) Climate change and marine plankton. *Trends Ecol Evol* 20: 337-344.

Holland, P.R. (2014), The seasonality of Antarctic sea ice trends. *Geophys Res Lett* 41, doi:10.1002/2014GL060172.

Hurwitz, B.L., Westveld, A.H., Brum, J.R., Sullivan, M.B. (2014) Modeling ecological drivers in marine viral communities using comparative metagenomics and network analyses. *PNAS* 111:10714-10719.

Kim, H., Doney, S.C. Iannuzzi, R.A., Meredith, M.P., Martinson, D.G., and Ducklow, H.W. (2016) Climate forcing for dynamics of dissolved inorganic nutrients at Palmer Station, Antarctica: An interdecadal (1993–2013) analysis. *J Geophys Res Biogeosci* 121:2369–2389. doi:10.1002/2015JG003311.

Kirchman, D.L., Morán, X.A., and Ducklow, H. (2009) Microbial growth in the polar oceans - role of temperature and potential impact of climate change. *Nat Rev Microbiol* 7:451-9.

Lebaron, P., Servais, P., Agogue, H., Courties, C., and Joux, F. (2001) Does the high nucleic acid content of individual bacterial cells allow us to discriminate between active cells and inactive cells in aquatic systems? *Appl Environ Microbiol* 67: 1775-1782.

Lenski, R.E. (1988) Dynamics of interactions between bacteria and virulent bacteriophage. *Adv Microb Ecol* 10: 1-44.

Longnecker, K., Sherr, B.F., and Sherr, E.B. (2005) Activity and phylogenetic diversity of bacterial cells with high and low nucleic acid content and electron transport system activity in an upwelling ecosystem. *Appl Environ Microbiol* 71: 7730-7749.

Marie, D., Partensky, F., Vaulot, D., and Brussaard, C.P.D. (1999) Enumeration of phytoplankton, bacteria, and viruses in marine samples. *Curr Protoc Cytom* 11: 1-15.

Meredith, M.P., and King, J.C. (2005) Rapid climate change in the ocean west of the Antarctic Peninsula during the second half of the 20th century. *Geophys Res Lett* 32: L19604.

Middelboe, M. (2000) Bacterial growth rate and marine virus-host dynamics. *Microb Ecol* 40: 114-124.

Middelboe, M., Jørgensen, N.O.G., and Kroer, N. (1996) Effects of viruses on nutrient turnover and growth efficiency of noninfected marine bacterioplankton. *Appl Environ Microbiol* 62: 1991-1997.

Mojica, K.D.A., and Brussaard, C.P.D. (2014) Factors affecting virus dynamics and microbial host-virus interactions in marine environments. *FEMS Microbiol Ecol* doi: 10.1111/1574-6941.12343.

Mojica, K.D.A., Evans, C., and Brussaard, C.P.D. (2014) Flow cytometric enumeration of marine viral populations at low abundances. *Aquat Microb Ecol* 71: 203-209.

Moline, M.A., Claustre, H., Frazer, T.K., Schofield, O., and Vernet, M. (2004) Alteration of the food web along the Antarctic Peninsula in response to a regional warming trend. *Glob Change Biol* 10:1973–1980.

Moline, M.A., and Prezelin, B.S. (1996) Palmer ITER 1991-1994: Long term monitoring and analyses of physical factors regulating variability in coastal antarctic phytoplankton biomass, *in situ* productivity and taxonomic composition over subseasonal, seasonal and interannual timescales. *Mar Ecol Prog Ser* 145: 143-160.

Montes-Hugo, M., Doney, S.C., Ducklow, H.W., Fraser, W., Martinson, D., Stammerjohn, S.E., and Schofield, O. (2009) Recent changes in phytoplankton communities associated with rapid regional climate change along the western Antarctic Peninsula. *Science* 323:1470-1473.

Moran, X.A.G., Estrada, M., Gasol, J.M., and Pedrós-Alió, C. (2002) Dissolved primary production and the strength of phytoplankton bacterioplankton coupling in contrasting marine regions. *Microb Ecol* 44: 217–223.

Murphy, E.J., Hofmann, E.E., Watkins, J.L., Johnston, N.M., Piñones, A., Ballerini, T., *et al*. (2013) Comparison of the structure and function of Southern Ocean regional ecosystems: The Antarctic Peninsula and South Georgia. *J Mar Syst* 109-110. 22-42.

Murray, A.G., and Jackson, C.A. (1992) Viral dynamics: a model of the effects of size, shape, motion and abundance of single-celled planktonic organisms and other particles. *Mar Ecol Prog Ser* 89: 103-116.

Oksanen, J., Blanchet, F.G., Kindt, R., Legendre, P., Minchin, P.R., O'Hara, R.B., Simpson, G.L., Solymos, P., Stevens, M.H.H., and Wagner, H. (2015) Multivariate Analysis of Ecological Communities in R: vegan tutorial. http://cran.r-project.org/web/packages/vegan/index.html

Ortega-Retuerta, E., Reche, I., Pulido-Villena, E., Agustí, S., Duarte, C.M. (2008) Exploring the relationship between active bacterioplankton and phytoplankton in the Southern Ocean. *Aquat Microb Ecol* 52: 99-106.

Pagarete, A., Chow, C-E.T., Johannessen, T., Fuhrman, J.A., Thingstad, T.F., and Sandaa, R.A. (2013) Strong seasonality and inter-annual recurrence in marine myovirus communities. *Appl Environ Microbiol* 79: 6253-6259.

Parsons, R.J., Breitbart, M., Lomas, M.W., and Carlson, C.A., (2012) Ocean time-series reveals recurring seasonal patterns of virioplankton dynamics in the northwestern Sargasso Sea. *ISME J* 6: 273-284.

Payet, J.P., and Suttle, C.A. (2008) Physical and biological correlates of virus dynamics in the southern Beaufort Sea and Amundsen Gulf. *J Mar Syst* 74: 933-945.

Pearce, I, Davidson, A.T., Bell, E.M., and Wright, S. (2007) Seasonal changes in the concentration and metabolic activity of bacteria and viruses at an Antarctic coastal site. *Aquat Microb Ecol* 47: 11–23.

Pomeroy, L.R., and Wiebe, W.J. (2001) Temperature and substrates as interactive limiting factors for marine heterotrophic bacteria. *Aquat Microb Ecol* 23:187-204.

Poorvin, L., Rinta-Kanto, J.M., Hutchins, D.A., and Wilhelm, S.W. (2004) Viral release of iron and its bioavailability to marine plankton. *Limnol Oceanogr* 49: 1734-1741.

Sheik, A.R., Brussaard, C.P.D., Lavik, G., Lam, P., Muscat, N., Krupke, A., *et al*. (2014) Responses of the coastal bacterial community to viral infection of the algae *Phaeocystis globosa*. *ISME J* 8:212-225.

Smith, R.C., Stammerjohn, S.E., and Baker, K.S. (1996) Surface air temperature variations in the western Antarctic peninsula region. In Foundations for ecological research west of the Antarctic Peninsula. Ross, R.M., Hofmann, E.E., and Quetin, L.B. (eds). American Geophysical Union, pp. 105–121.

Stammerjohn, S.E., Martinson, D.G., Smith, R.C., Iannuzzi, R.A. (2008) Sea ice in the western Antarctic Peninsula region: Spatio-temporal variability from ecological and climate change perspectives. *Deep-sea Res II* 55: 2041-2058.

Stammerjohn, S.E., Massom, R., Rind, D. and Martinson, D. (2012) Regions of rapid sea ice change: An inter-hemispheric seasonal comparison. *Geophys Res Lett* 39: L06501, doi:10.1029/2012GL050874.

Suttle, C.A. (2005) Viruses in the sea. *Nature* 437: 356-361.

Suttle, C.A. (2007) Marine viruses - major players in the global ecosystem. *Nat Rev Microbiol* 5: 801-812.

Thingstad, T.F. (2000) Elements of a theory for the mechanisms controlling abundance, diversity, and biogeochemical role of lytic bacterial viruses in aquatic systems. *Limnol Oceanogr* 45: 1320–1328.

Thingstad, T.F. and Lignell, R. (1997) Theoretical models for the control of bacterial growth rate, abundance, diversity and carbon demand. *Aquat Microb Ecol* 13: 19-27.

Thomson, P.G., Davidson, A.T., van den Enden,R., Pearce, I., Seuront, L., Paterson, J.S., and Williams, G.D. (2010) Distribution and abundance of marine microbes in the Southern Ocean between 30 and 80°E. *Deep Sea Res Part II* 57: 815-827.

Vaughan, D.G., Marshall, G.J., Connolley, W.M., Parkinson, C., Mulvaney, R., Hodgson, D.A., *et al*. (2003) Recent rapid regional climate warming on the Antarctic Peninsula. *Clim Chang* 60: 243-274.

Venables, H.J., Clarke, A., and Meredith, M.P. (2013) Wintertime controls on summer stratification and productivity at the western Antarctic Peninsula. *Limnol Oceanogr* 58: 1035-1047.

Vernet, M., Martinson, D., Iannuzzi, R., Stammerjohn, S., Kozlowski, W., Sines, K., *et al*. (2008) Primary production within the sea-ice zone west of the Antarctic Peninsula:I—Sea ice, summer mixed layer, and irradiance. *Deep Sea Res II* 55: 2068– 2085.

Weinbauer, M.G. (2004) Ecology of prokaryotic viruses. *FEMS Microbiol Rev* 28: 127-181.

Weinbauer, M.G., and Holfe, M.G. (1998) Significance of viral lysis and flagellates grazing as factors controlling bacterioplankton production in a eutrophic lake. *Appl Environ Microbiol* 64:431–438.

Wilhelm, S.W., and Suttle, C.A. (1999) Viruses and nutrient cycles in the sea. *Bioscience* 49: 781-788.

Winget, D.M., Helton, R.R., Williamson, K.E., Bench, S.R., Williamson, S.J., and Wommack, K.E. (2011) Repeating patterns of virioplankton production within an estuarine ecosystem. *Proc Natl Acad Sci U S A* 108: 11506-11511.

Zhao, Y., Temperton, B., Thrash, J.C., Schwalbach, M.S., Vergin, K.L., Landry, Z.C., *et al*. (2013) Abundant SAR11 viruses in the ocean. *Nature* 494: 357-360.

Zubkov, M.V., Fuchs, B., Burkill, P.H., and Amann, R. (2001) Comparison of cellular and biomass specific activities of dominant groups in stratified waters of the Celtic Sea. *Appl Environ Microbiol* 67: 5210-5218.

Figure legends

Figure 1: Map of the local area and Rothera Time Series (RaTS) sampling sites. Adelaide Island is located west of the Antarctic Peninsula and bordered to the south by Marguerite Bay. The sampling sites RaTS 1 and RaTS 2 are located to the southwest of the British Antarctic Survey's Rothera Research Station at respectively 67.570ºS 68.225ºW and 67.581ºS 68.156ºW.

Figure 2: Weekly averages of the environmental conditions during the 8-year sampling period (A-G) and the number of samples (summed total over the time series) available for each week of the year (H). Water temperature (A) and salinity (C) were measured by CTD at a depth of 15 m; the mixed layer depth (D) was also measured by CTD, whereas the level of ice cover in the bay (B) was assessed visually (from 1 = ice-free conditions to 6 = fast ice), on some occasions from the base rather than on-site. Levels of the dissolved inorganic nutrients NOx (E), phosphorous (F) and silicate (G) were determined in the lab from water samples taken at 15 m depth. Plots A to G show both the range (shaded) and median value (solid line) of measurements during each calendar week.

Figure 3: Time series of the environmental conditions during the 8-year sampling period from mid-2002 to early 2011. Water temperature (A), salinity (C) and levels of photosynthetically active radiation (E) were measured by CTD at a depth of 15 m; the mixed layer depth (D) was also measured by CTD, whereas the level of ice cover in the bay (B) was assessed visually (see main text for scale explanation). Levels of the dissolved inorganic nutrients NOx (E), phosphorous (F) and silicate (G) were determined in the lab from water samples taken at 15 m depth. The shading in each graph indicates the "winter" season as defined by local and region sea ice cover, which was used to subdivide the time series data for statistical analyses (see main text and Supplementary Materials).

Figure 4: Weekly averages of the plankton abundances during the 8-year sampling period (A-E) and the number of samples (summed total over the time series) available for each week of the year (F). Chlorophyll concentrations (A) and abundances of total bacterioplankton (B) and virioplankton (C), as well as relative abundances of bacterial (D) and viral subgroups (E), were determined in the lab from water samples taken at 15 m depth. Plots A to D show both the range (shaded) and median value (solid line) of measurements during each calendar week, whereas E shows only the median values.

Figure 5: Time series of the plankton abundances during the 8-year sampling period from mid-2002 to early 2011, as determined in the lab from water samples taken at 15 m. Chlorophyll concentrations (A) are broadly representative of phytoplankton levels. Total bacterioplankton (B), %HNA bacteria (C), virus-to-bacteria ratio (VBR; D), total virioplankton (E), and viral subgroups (V1-V3; F-H) were enumerated by flow cytometry. The shading in each graph indicates the “winter” season as defined by local and region sea ice cover (see main text and Supplementary Materials). No bacterioplankton or virioplankton data are available from March 2007 to March 2008 owing to loss of the samples collected during this period.

Figure 6: Principal Coordinates Ordination (PCO) of the Euclidian distance of the plankton abundances (chlorophyll, V1, V2 and V3 viruses, and HNA and LNA bacteria) during each summer (black circles) and winter (white diamonds) of the time series (e.g. “S0607” represents the summer season of 2006 to 2007). Note that the PCO of a Euclidian distance-based matrix is equivalent to a Principal Component Analysis. The way in which the biological and physicochemical data relate to the PCO (Pearson’s r) is illustrated with the adjacent vector plot: the direction of each vector reflects the direction of increase of the variable (i.e., higher number or magnitude), whereas the vector length represents the strength of the correlation (i.e., between the variable and the distribution of the biological data). Abbreviations used: Chlorophyll (Chl); bacteria subgroups (HNA, LNA); viral subgroups (V1-V3); temperature (T);

salinity (Sal); ice cover (Ice); mixed layer depth (MLD); phosphorous (P); nitrogen oxides (NOx); silicate (Si).

Figure 7: Distance-based Redundancy Analysis (dbRDA) plot of the distance-based linear mixed model (distLM in PRIMER) fitted to the variation in plankton abundances. The model was constructed using a combination of the Akaike Information Criterion (AIC) and a forward selection procedure to select the most significant and useful predictor variables (in red): salinity (Sal), phosphorous (P), silicate (Si) and NOx.

Figure 8: Abundances of HNA bacteria and viral group V1 during February and March 2010, illustrating their co-variation.

Supplementary materials

Subdivision of the time series into seasonal segments for data exploration and statistical analyses

Whilst attempting to find correlations and trends in the high-resolution RaTS time series data set, two issues were initially identified. The first was the relatively high prevalence of 'missing' and 'misaligned' data. Reasons for this varied, but included measurements and/or samples not being taken, lost, or not recorded, or for example water samples for nutrient concentrations and plankton abundances being collected on different days. This results in incomplete rows of data, which need to be either filled in using any of a number of data imputation strategies, or deleted before statistical comparison. The second issue was the magnitude of change between summer and winter conditions, which for all measured parameters was much higher than the year-to-year variation, as is typical for high latitude marine ecosystems. This trend causes the seasonality to mask any underlying functional correlations within the data. To omit the seasonality issue and simultaneously preserve the entire data set, we therefore decided to subdivide the time series into a smaller number of discrete time segments (reflecting "summer" and "winter" conditions), and for each parameter calculate a single integrated value for each time segment (area under curve). This condensed data set was then used to describe the interannual variability in plankton abundances and to model which physicochemical parameters are driving this variability.

To define the boundaries between the "summer" and "winter" time segments, an independent criterion was sought. Previous studies by Stammerjohn *et al*. (2008; 2012) used satellite observations to define the dates of sea ice advance and retreat around Antarctica. We compared sea ice data from the wider region (Marguerite Bay) as measured by satellite, to the visual assessment of local sea ice cover in Ryder Bay (on a scale of 1 to 6, 1 being ice-free and 6 being fast ice). A local sea ice cover score of 4 or higher for more than one week corresponded very well with a regional sea ice onset threshold of more than 50% cover derived from the satellite image, whereas a local cover score of 3 or lower corresponded with

a regional retreat threshold of less than 50% cover. As the dates correspond very well in both cases, the local sea ice score was chosen as the independent criterion for subdivision of the time series.

[insert figure S1 – sea ice assessment]

Figure S1: Day of (A) sea ice onset using a visual assessment score for Ryder Bay of 4 or higher for more than one week (red line), and a value of more than 50% cover in the Marguerite Bay satellite image (blue line); and B) sea ice retreat a visual assessment score for Ryder Bay of 3 or less (red line), and a value of less than 50% cover in the Marguerite Bay satellite image (blue line). In both cases the dates were normalized to the 1st of January as day 1.

Flow cytometry

Flow cytometry has gained popularity as a method to quantify viruses from aquatic systems due to its high sample throughput and ability to distinguish several viral subpopulations. Comparison of flow cytometric viral counts with those generated by epifluorescence microscopy generally yield complete agreement indicating the method is accurate and standard deviations for replicate samples are typically below 5% confirming high levels of precision (Brussaard *et al*., 2010). Furthermore, virioplankton counts generated by flow cytometry are unlikely to be perturbed by bacterial vesicles present in seawater since vesicles have comparatively much smaller associated DNA fragments, typically around 3 kilobase pairs (Biller *et al*., 2014), thus generating insufficient green fluorescence after staining to be detected by flow cytometry (Brussaard *et al*., 2010). N.B. typically even the small genome marine viruses have a genome size an order of magnitude larger than the vesicles (e.g. Steward *et al*., 2000). Therefore, it is unlikely that vesicles contributed significantly to LNA prokaryotes or the viral subgroups detected during our study.

[insert figure S2 – flow cytometry]

Wiley-Blackwell and Society for Applied Microbiology

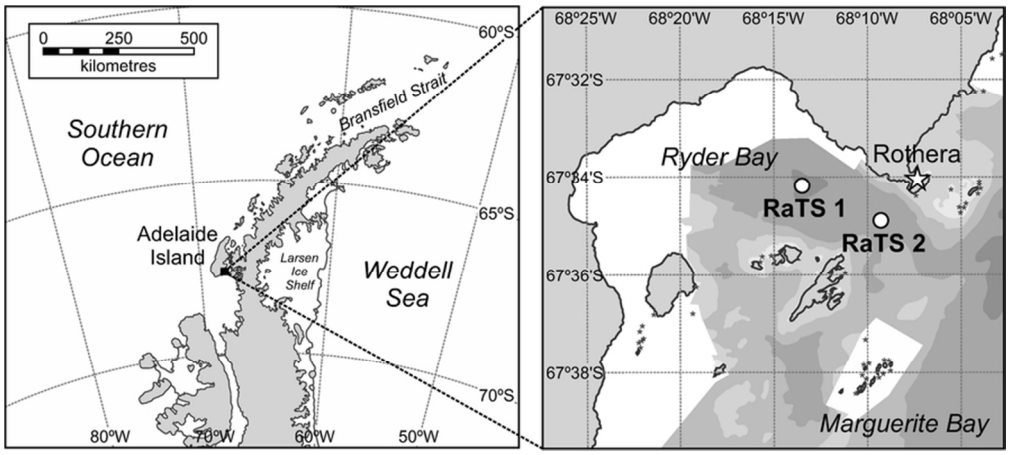

Map of the local area and Rothera Time Series (RaTS) sampling sites. Adelaide Island is located west of the Antarctic Peninsula and bordered to the south by Marguerite Bay. The sampling sites RaTS 1 and RaTS 2 are located to the southwest of the British Antarctic Survey's Rothera Research Station at respectively 67.570ºS 68.225ºW and 67.581ºS 68.156ºW.

[insert figure 1 - map]

75x33mm (300 x 300 DPI)

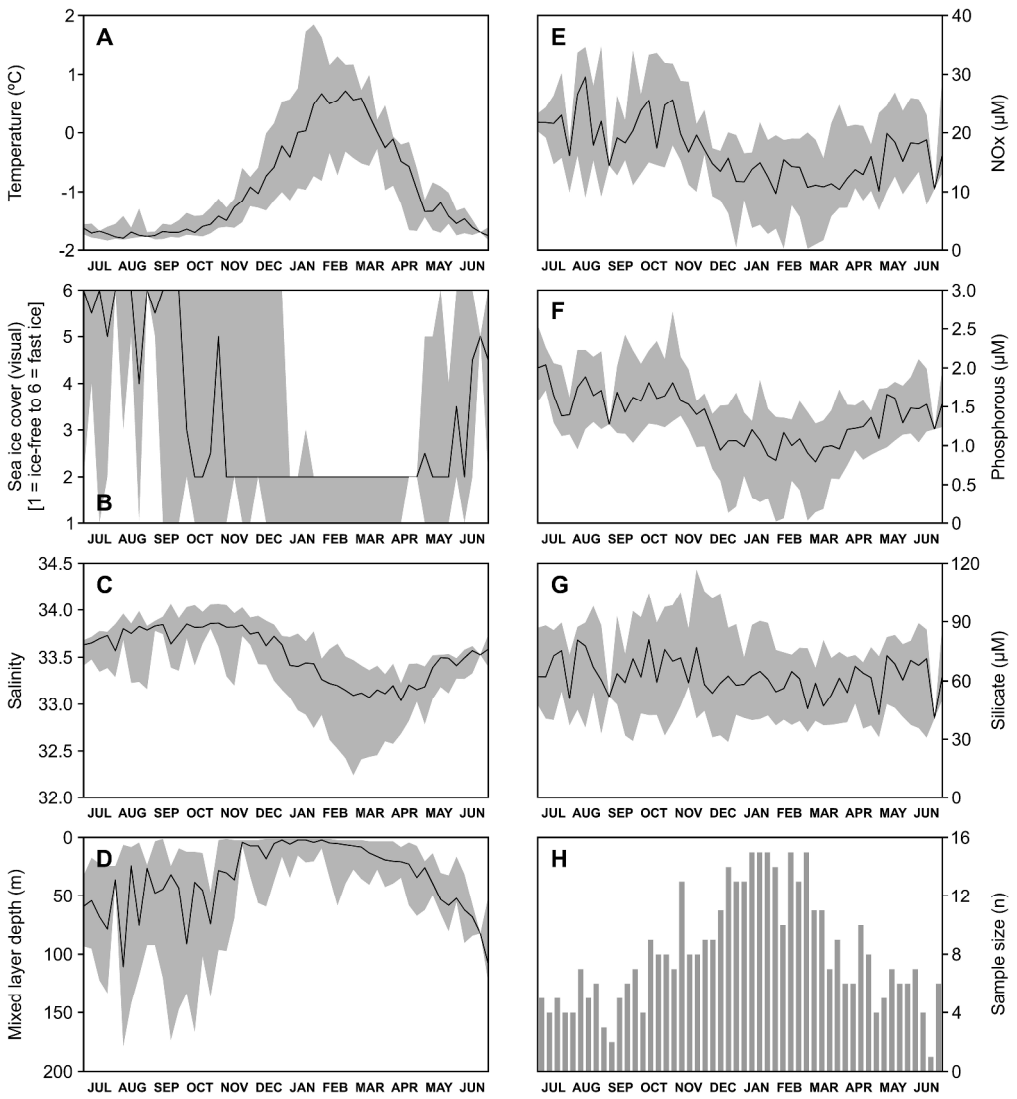

Weekly averages of the environmental conditions during the 8-year sampling period (A-G) and the number of samples (summed total over the time series) available for each week of the year (H). Water temperature (A) and salinity (C) were measured by CTD at a depth of 15 m; the mixed layer depth (D) was also measured by CTD, whereas the level of ice cover in the bay (B) was assessed visually (from 1 = ice-free conditions to 6 = fast ice), on some occasions from the base rather than on-site. Levels of the dissolved inorganic nutrients NOx (E), phosphorous (F) and silicate (G) were determined in the lab from water samples taken at 15 m depth. Plots A to G show both the range (shaded) and median value (solid line) of measurements during each calendar week.

[insert figure 2 – physicoch
389x423mm (300 x 300 DPI)

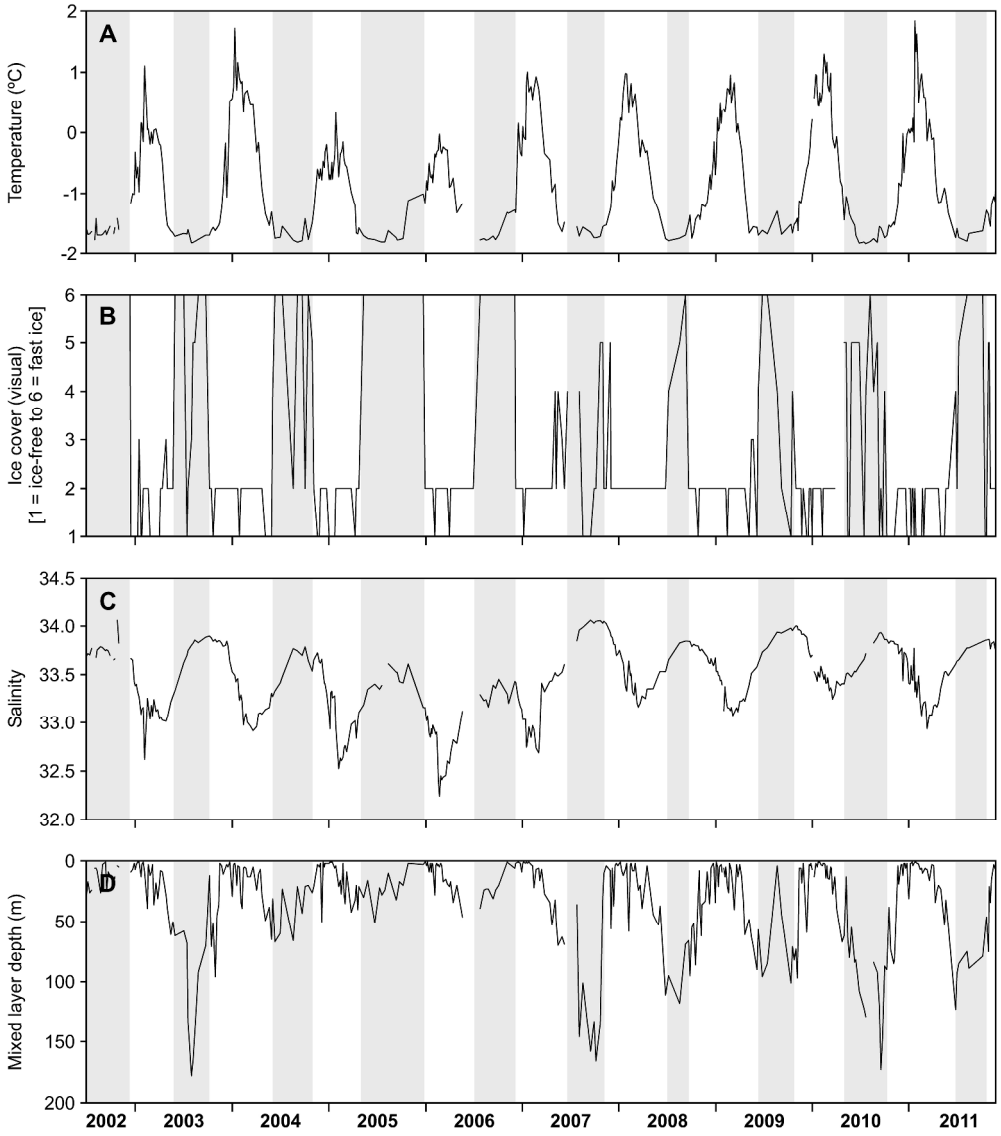

[insert figure 3_part 1 – ph
390x441mm (300 x 300 DPI)

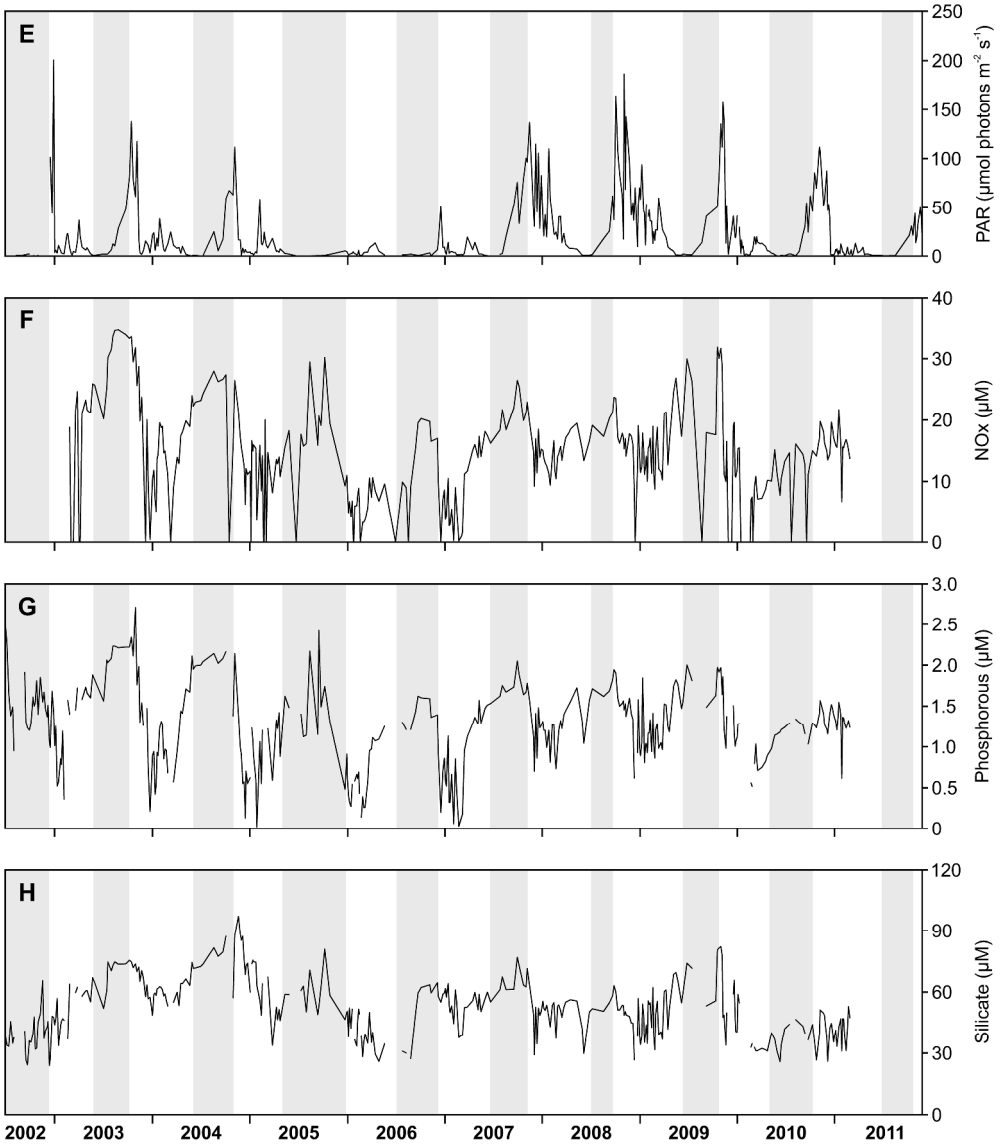

Time series of the environmental conditions during the 8-year sampling period from mid-2002 to early 2011. Water temperature (A), salinity (C) and levels of photosynthetically active radiation (E) were measured by CTD at a depth of 15 m; the mixed layer depth (D) was also measured by CTD, whereas the level of ice cover in the bay (B) was assessed visually (see main text for scale explanation). Levels of the dissolved inorganic nutrients NOx (E), phosphorous (F) and silicate (G) were determined in the lab from water samples taken at 15 m depth. The shading in each graph indicates the "winter" season as defined by local and region sea ice cover, which was used to subdivide the time series data for statistical analyses (see main text and Supplementary Materials).

[insert figure 3_part 2 – ph
390x444mm (300 x 300 DPI)

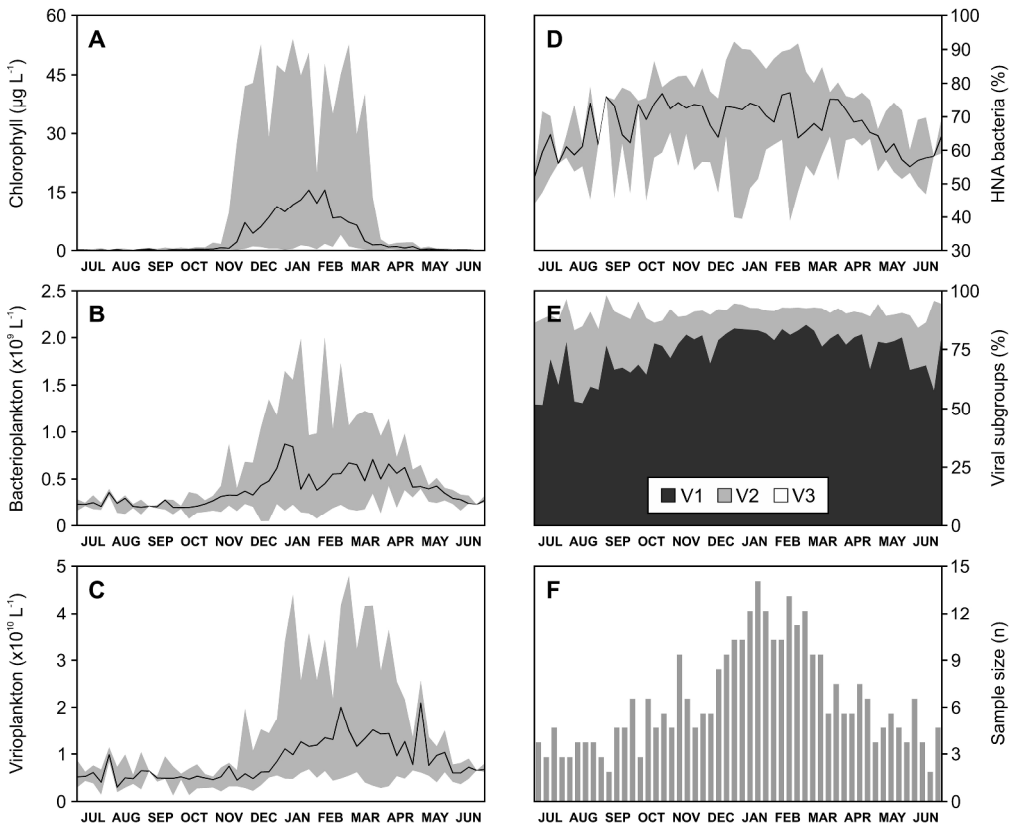

Weekly averages of the plankton abundances during the 8-year sampling period (A-E) and the number of samples (summed total over the time series) available for each week of the year (F). Chlorophyll concentrations (A) and abundances of total bacterioplankton (B) and virioplankton (C), as well as relative abundances of bacterial (D) and viral subgroups (E), were determined in the lab from water samples taken at 15 m depth. Plots A to D show both the range (shaded) and median value (solid line) of measurements during each calendar week, whereas E shows only the median values.

[insert figure 4 – biology a
291x238mm (300 x 300 DPI)

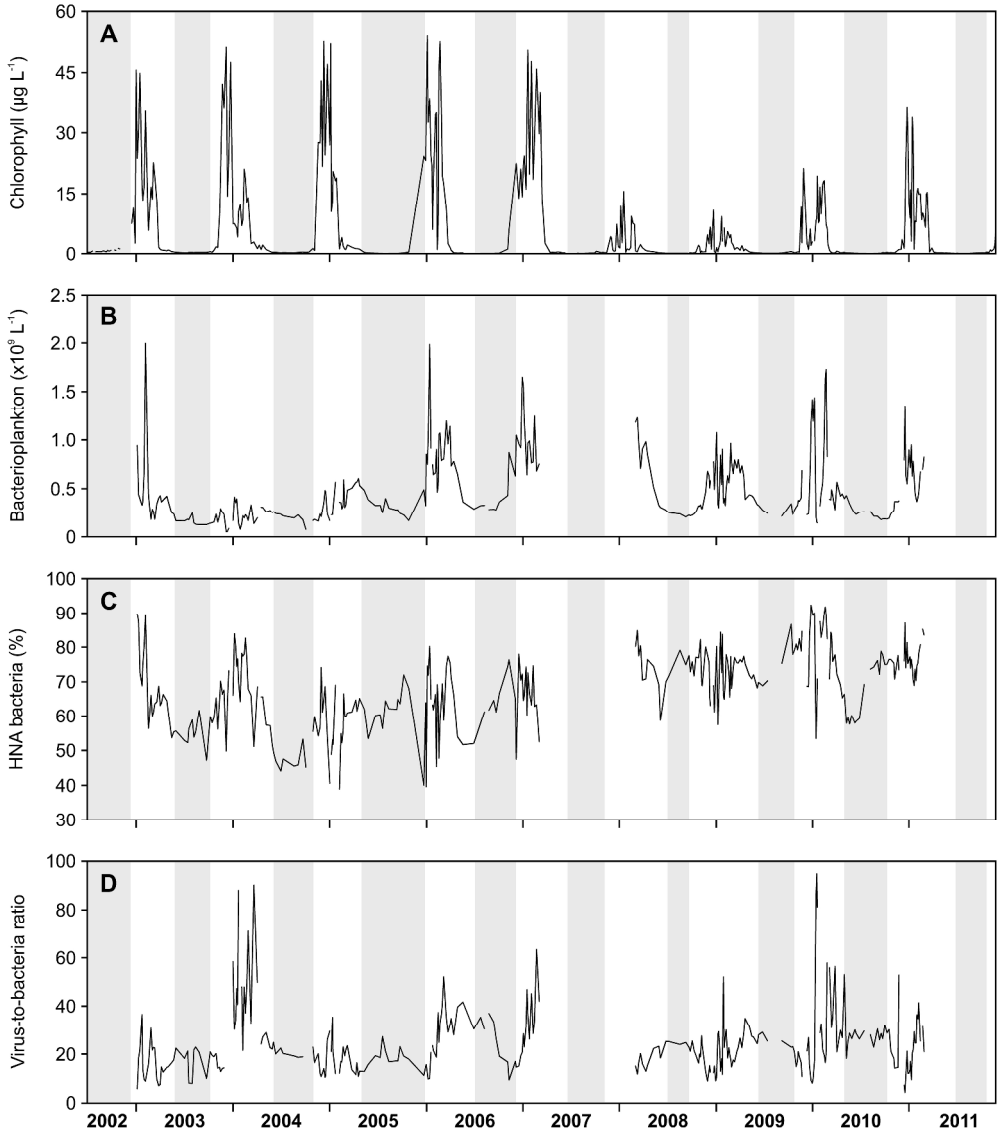

[insert figure 5_part 1 – bi
390x440mm (300 x 300 DPI)

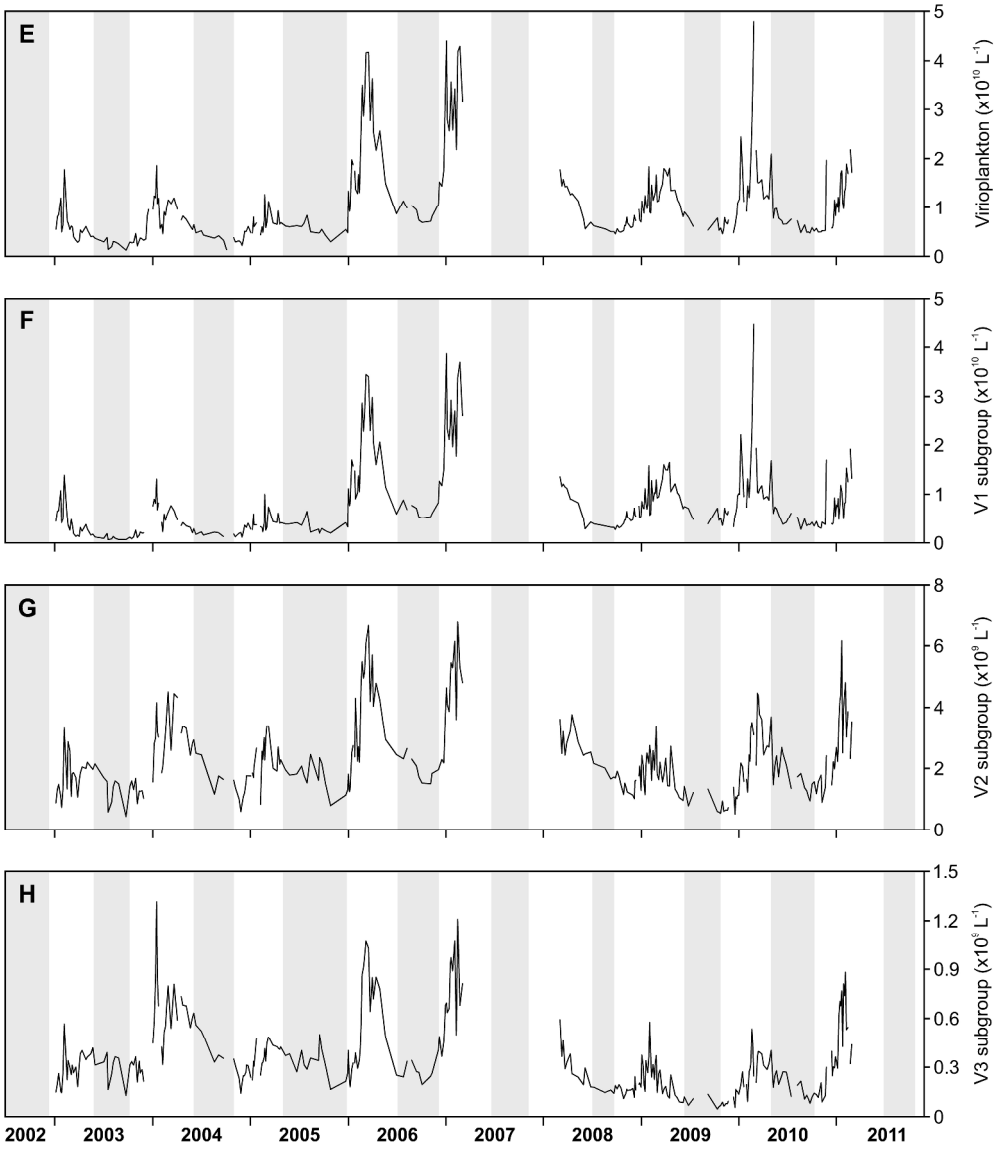

Time series of the plankton abundances during the 8-year sampling period from mid-2002 to early 2011, as determined in the lab from water samples taken at 15 m. Chlorophyll concentrations (A) are broadly representative of phytoplankton levels. Total bacterioplankton (B), %HNA bacteria (C), virus-to-bacteria ratio (VBR; D), total virioplankton (E), and viral subgroups (V1-V3; F-H) were enumerated by flow cytometry. The shading in each graph indicates the "winter" season as defined by local and region sea ice cover (see main text and Supplementary Materials). No bacterioplankton or virioplankton data are available from March 2007 to March 2008 owing to loss of the samples collected during this period.
[insert figure 5_part 2 – bi
390x445mm (300 x 300 DPI)

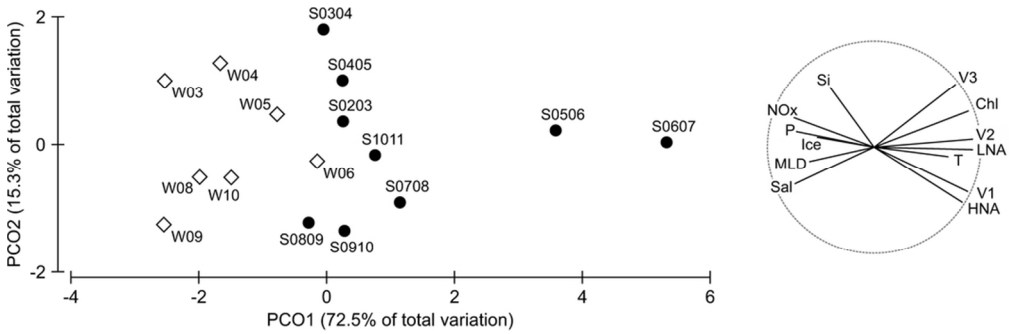

Principal Coordinates Ordination (PCO) of the Euclidian distance of the plankton abundances (chlorophyll, V1, V2 and V3 viruses, and HNA and LNA bacteria) during each summer (black circles) and winter (white diamonds) of the time series (e.g. "S0607" represents the summer season of 2006 to 2007). Note that the PCO of a Euclidian distance-based matrix is equivalent to a Principal Component Analysis. The way in which the biological and physicochemical data relate to the PCO (Pearson's r) is illustrated with the adjacent vector plot: the direction of each vector reflects the direction of increase of the variable (i.e., higher number or magnitude), whereas the vector length represents the strength of the correlation (i.e., between the variable and the distribution of the biological data). Abbreviations used: Chlorophyll (Chl); bacteria subgroups (HNA, LNA); viral subgroups (V1-V3); temperature (T); salinity (Sal); ice cover (Ice); mixed layer depth (MLD); phosphorous (P); nitrogen oxides (NOx); silicate (Si).
[insert figure 6 - PCO]
89x28mm (300 x 300 DPI)

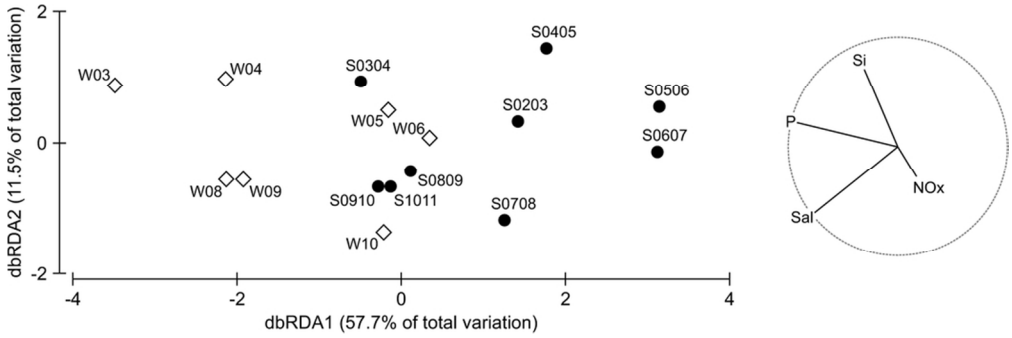

Distance-based Redundancy Analysis (dbRDA) plot of the distance-based linear mixed model (distLM in PRIMER) fitted to the variation in plankton abundances. The model was constructed using a combination of the Akaike Information Criterion (AIC) and a forward selection procedure to select the most significant and useful predictor variables (in red): salinity (Sal), phosphorous (P), silicate (Si) and NOx.
[insert figure 7 – distLM mo
88x29mm (300 x 300 DPI)

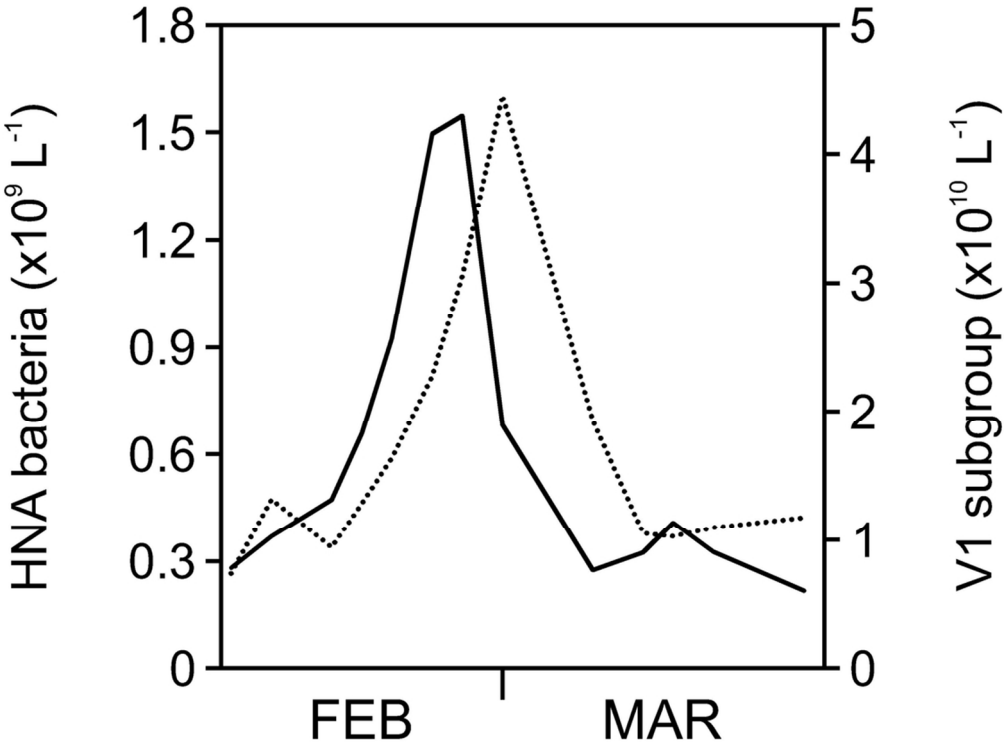

Abundances of HNA bacteria and viral group V1 during February and March 2010, illustrating their co-variation.
[insert figure 8 – HNA and V
97x72mm (300 x 300 DPI)